DSP Based Power Quality Analyzer

Pedro A. Xavier[1], Pedro M. Ramos[1]

[1] Instituto Superior Técnico, Universidade Técnica de Lisboa, Lisbon, Portugal
email: peaxavier@gmail.com, pedro.ramos@lx.it.pt

Abstract *– This paper presents a system designed for real-time detection and classification of power quality (PQ) voltage disturbances in a continuously monitored single-phase power system. The following methods were implemented in a DSP-based analyzer: sine-fitting, multiharmonic fitting and closing morphological operation are used to detect transient and waveform distortions and for short and long duration disturbances (such as sags, swells, and interruptions) the analysis of the root mean square (RMS) value of the voltage is employed.*

Keywords *- Power Quality Analyzer, Digital Signal Processor, Detection and Classification of Disturbances, Sine-Fitting, Closing Morphological Operation.*

I. INTRODUCTION

In recent years, multiple challenges appeared in the area of energy for producers, electricity distributors and consumers. The growing concern with environment, energy, and financial savings lead energy consumers to the urgent need for modern, efficient, and intelligent systems to monitor the electrical grid and improve power quality and its management. A network monitoring system enables providers to detect electrical anomalies (and their causes) and thus provide a better energy service to the community, saving countless recurring losses from the effects of disturbances. Among these are material damages, deterioration of the lifetime of the equipment and loss of information.

One of the main causes for the lack of quality in electrical systems is the increased use of electronic equipment that causes and is, at the same time, susceptible to a variety of electromagnetic interference and phenomena that characterizes voltages and current waveforms in time. Although the power grid has suffered a recent modernization mainly due to the new possibilities offered by decentralized generation and power electronics that result in more efficient and safer ways of power distribution, power quality disturbances continue to occur with severe implications, both in domestic and industrial equipment. Thus, power quality remains a matter of extreme importance not only for electrical engineers in particular but to all in general.

Since deterioration of power quality is a concern, low-cost systems that provide continuous monitoring of power quality are needed. These devices are called power quality analyzers and aim to:

- Detect and classify, almost instantaneously, a wide variety of electrical disturbances;
- Store in external memory devices (like SD memory cards) the main characteristics of the disturbance: type, time of occurrence, magnitude, etc.;
- Transmit stored data remotely (Ethernet) or localy (RS-232, USB, Blutooth, etc.);
- Ensure quality of service (QoS) levels required by regulating entities (*e.g.*, in Portugal, ERSE [1]).

A. Work Goals

The goal of this project is to develop, implement and characterize a prototype with the functionality of power quality analyzer in a low voltage single-phase power system in which real-time detection and classification algorithms of PQ events are implemented. The PQ analyzer is based on a digital signal processor (DSP) which provides computational power to perform complex signal algorithms. A redundant power supply provides all voltage and current signals required by the system, and if there is a power interruption in the main power grid, a Li-Ion battery is used while the power is not restored.

The prototype is meant to be installed in a power station on the street, only accessed by employees of electricity distributors company. To this end, the analyzer performs a detailed analysis of the power grid's voltage signal and its eventual disturbances in real-time. The detection and classification of disturbances should be a reliable process so that their causes can be identified.

B. State of Art

According to IEEE 1159-1995 [2] standard, the PQ disturbances can be divided into the following categories: sags, swells, interruptions, transients, undervoltages, and overvoltages and waveform distortions (*e.g.*, harmonics and noise). In Table 1 the ten most common categories of disturbances encountered in a single-phase power system are presented together with their main characteristics.

Table 1 – Categories of PQ disturbances and their typical parameters as defined in [2].

Category	Typical Duration	Typical magnitude
Transient (up to 5 MHz)	ns - ms	0 - 8 p.u.
Harmonics (0 to 9 kHz)	Steady state	0 – 0.2 p.u.
Inter-harmonics (0 to 9 kHz)	Steady state	0 – 0.02 p.u.
Notching	Steady state	
Noise (broad-band)	Steady state	0 – 0.01 % p.u.
Sag	0.5 cycle - 1 min	0.1 – 0.9 p.u.
Swell	0.5 cycle - 1 min	1.1 – 1.8 p.u.
Interruption	> 0.5 cycle	< 0.1 p.u.
Undervoltage	> 1 min	0.8 – 0.9 p.u.
Overvoltage	> 1min	1.1 – 1.2 p.u.

Several approaches for automatic detection and classification of PQ disturbances have been proposed. The process is often based on time-frequency representations such as wavelet transform [3] or the short-time Fourier transform [4], which are assisted by neural networks [5], [3] or fuzzy expert systems. Methods based on patter recognition using support vector machines are also useful techniques for disturbance classification [6]. Other approaches apply a bank

of digital filters [7] or the calculation of the voltage root-mean square (RMS) value [8].

II. SYSTEM'S ARCHITECTURE

The PQ analyzer (Figure 1) uses a closed-loop Hall effect transducer to measure the voltage in a single-phase 230 V/50 Hz power system. The voltage transducer *LEM*© LV 25-P has an input range of ± 500 V and bandwidth 30 kHz. The output signal of the transducer is processed by a signal conditioning circuit and digitized using a successive approximation analog-to-digital converter (A/D). Its sampling rate is set to 25.6 kS/s and the resolution is 16 bits. The sampling clock of the A/D (AD7980 of *Analog Devices*©) is generated by the digital signal processor ADSP-21369 of *Analog Devices*©. The DSP uses its internal precision clock generator to produce a stable and low-jitter sampling clock. The A/D is connected to one of the DSP's synchronous serial ports (SPORT). Besides controlling the data acquisition process, the DSP also performs all the processing required by the proposed algorithm for detection and classification of disturbances. The selected DSP is a 32-bit floating point processor running at 332 MHz. The DSP has 2 Mbit of internal memory capacity. Since this is not sufficient to store all data and to perform all the required processing, a 128 Mbit synchronous dynamic RAM (SDRAM) is connected to the DSP. The SDRAM memory is used to store auxiliary data and variables required during the processing and to store the acquired data while it is processed. Associated to each disturbance is a set of features such as the time of occurrence, magnitude and duration. To measure the time of every instant there is a real-time clock which is controlled through I^2C protocol.

When the PQ analyzer is connected to a PC, the detected disturbances characteristics can be uploaded via UART interface (RS-232 protocol). When there's a connection, the PC is running a program implemented in *LabVIEW*© to receive and store the data sent by the processor.

The PQ analyzer must be able to work even when the voltage in the power network is outside its nominal range. Since the analyzer is powered from the monitored power system, it contains a backup rechargeable Li-Ion battery which is used to power the analyzer during interruptions or sags. The battery is recharged when needed and the voltage in the power system is at its nominal level. The power supply provides battery backed-up power for all the analyzer's electronics and for the voltage transducer.

A. Voltage Transducer LEM LV 25-P

The schematic with the voltage transducer and its connections to the power grid, resistors and power supply is shown in Figure 2. For voltage measurements, a current proportional to the measured voltage must pass go an external resistor R0 which is connected in series with the transducer's primary circuit. The output voltage is measured at resistor RM. Both resistors were dimensioned considering the abnormal situation of 460 V RMS in the power line. This last consideration is intended to protect all components and allow a greater range of voltage to be measured (*e.g.*, to measure overvoltages). Although a more economic solution could be chosen instead of the voltage transducer (*e.g.*, voltage divider), the transducer offers other characteristics that a voltage divider don't, like excellent accuracy, good linearity, low thermal drift, high bandwidth, isolation and immunity to external interference.

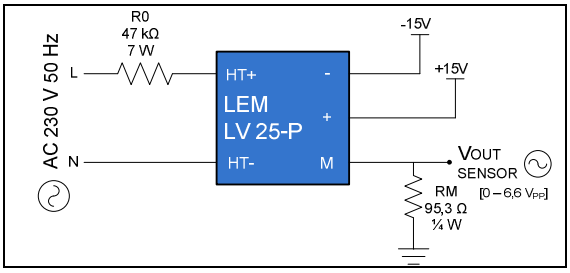

Figure 2 – Schematic of the voltage transducer's connections.

B. Signal Conditioning Circuit

Given that the A/D accepts only positive voltages and the signal at the output of the voltage transducer is bipolar, it was necessary to implement a signal conditioning circuit. This circuit, presented in Figure 3 was designed to transform a bipolar signal into a one with positive polarity and within the range of voltages allowed by the A/D (0 to 3.3 V).

When the grid voltage is a sinusoidal signal with 460 V RMS, the signal conditioning circuit output is a sine signal centered at 1.65 V and with magnitude 3.3 V. The output/input relation of the signal conditioning is

$$V_{OUT} = 1.65 - 0.5 \cdot V_{IN}. \quad (1)$$

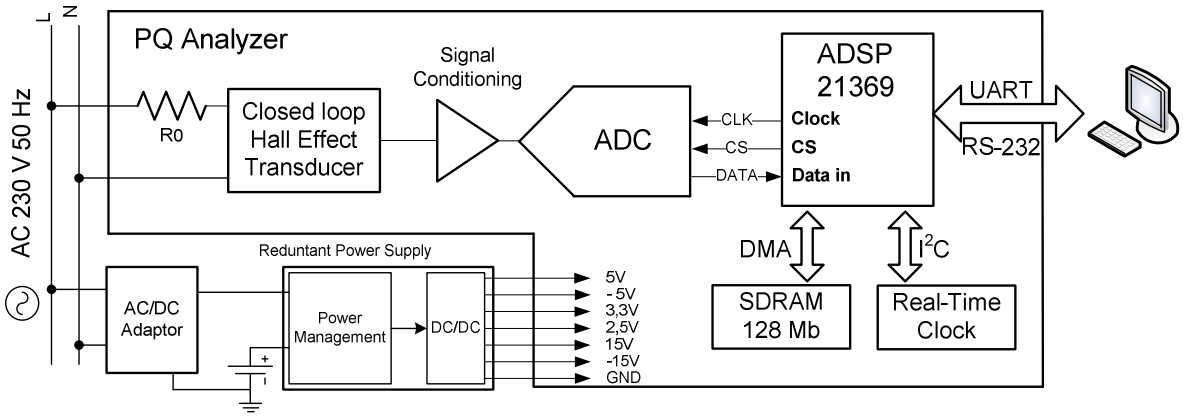

Figure 1 - Block diagram of the proposed PQ analyzer

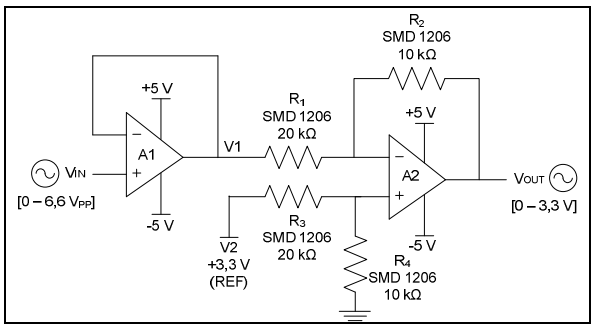

Figure 3 – Conditioning circuit schematic.

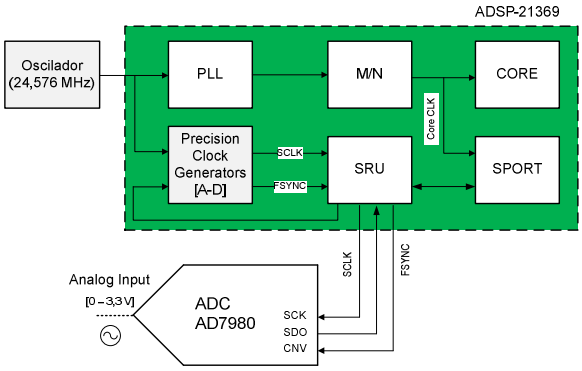

Figure 5 - PCG clock signals to control the A/D.

C. *Analog to Digital Converter AD7980*

Before the sampling process, the signal is filtered by a low-pass filter (Figure 4), whose cutoff frequency f_C is 14 kHz. This filter reduces noise, preserves SNR and avoids aliasing. The A/D receives the analog signal in the IN+ input pin whose range should be between 0 and 3.3 V (V_{REF}). Due to the maximum voltage allowed in SDO (data), SCK (clock) and CNV (chip select) pins (referenced to DSP), the SDI and VIO pins are connected to 3.3 V. The communication between the DSP and the converter is done through SPI. The A/D is powered with 3.3 V (VIO for the digital interface) and 2.5 V (VDD for the analog part). A voltage reference of 3.3 V is connected to REF.

The DSP has four precision clock generators (PCG). Each of them has a set of signals (clock and frame sync) derived from a master clock. It is the internal phased locked loop (PLL) that generates the clock for the processor and also generates clock signals for the SPORTs (Figure 5). However, generating clock signals from the PLL to the serial ports isn't recommended when converting an analog signal to a digital one because this solution may create problems related to jitter, which typically arises when there is more than one clock frequency involved. Since the processor operates at a high frequency, signal integrity, noise problems and errors of measurement should be considered.

The solution to avoid jitter is generating the clock signals from the PCGs. The PCGs are directly connected to a precision external oscillator rather than the PLL, as shown in Figure 5. This crystal oscillates at 24.576 MHz and is a reference to all clock signals (UART's transfer rate, memory access rate, etc.).

D. *External Memory (SDRAM)*

Due to the insufficient capacity of the internal memory to store all samples needed for signal analysis and process all required algorithms, an external SDRAM memory with 128 Mbit was included. This memory is organized in four banks of 32 Mbit, each with 4096 rows by 256 columns and 32 bit.

When the internal buffer reaches its maximum capacity, the acquired data is immediately transferred through DMA to an address in the external memory. The DMA transfer of large sets of words (the size of the internal buffer) is ideal for real-time operations since the memory access is done directly, regardless the state of the central processing unit. Its simplicity resides in just setting the reading/writing base address and activating the transfer.

While the DMA transfer takes place, whether in writing or reading, the processor is carrying out other operations. This is one of the main advantages of using DMA, concurrent operations do not wait until the transfer is over to execute. The acquisition of multiple samples and their transfer to the external memory in blocks, makes the process much more quicker than sending samples one by one. This way the use of the external SDRAM is optimized (efficiently use the SDRAM's speed) as well the overall performance of the analyzer.

E. *Real-Time Clock (RTC)*

When disturbances occur it's necessary a continuous temporal record so that the time of occurrence could be registered. In this way, a real-time clock (RTC) is required.

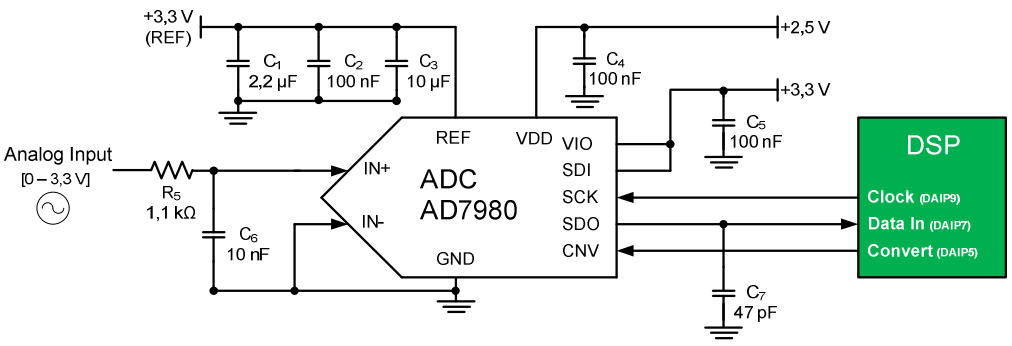

Figure 4 - Schematic of the A/D converter.

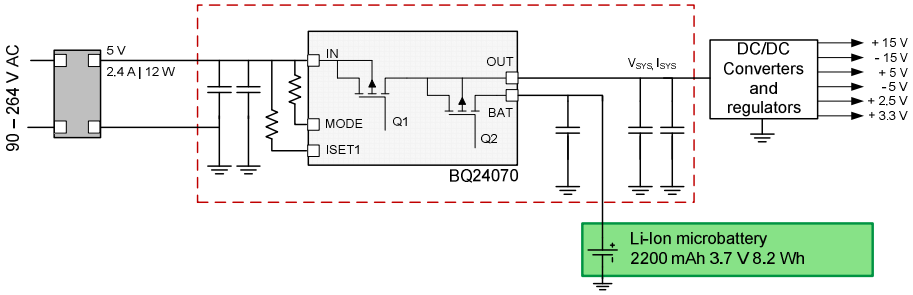

Figure 1 - Block diagram of the redundant power supply.

The RTC chosen is the M41T81S of *STMicrolectronics*©. This RTC is able to count tens of milliseconds, seconds, minutes, hours, days, months, years and centuries. The communication between the processor is done by using I^2C protocol. The format of the numbers is the binary coded decimal (BCD) in which 8 bytes of internal SRAM are for clock/calendar functions and 12 bytes for reading the status of integrated control or timer registers.

The RTC is powered with 3.3 V. In case of power failure the RTC has also a coin battery attached (model BR1225, 3 V and 48 mAh) for backup power. According to application note AN1012 of *STMicroelectronics*©, the lifetime of the battery can go from 300 h to 1800 h depending on the load associated with it.

F. Redundant Power Supply

The redundant power supply designed for this work should be able to power the system (voltage sensor, ADC, SDRAM, RTC, etc.) even when there are interruptions or sags in the electrical grid. Therefore, the power supply must carry a backup battery to supply the system when those disturbances occur.

The block diagram of the power supply is illustrated in Figure 1. There is an AC/DC converter that provides a fixed output voltage of 5 V and 2.4 A (max.) to the power-path energy management chip (BQ24070) of *Texas Instruments*©. This integrated circuit is responsible for charging and Li-Ion battery when needed and simultaneously supply DC/DC converters and voltage regulators. Their mission is to provide several voltage levels and currents to the components of the power quality analyzer.

III. SYSTEM'S ALGORITHMS

The method of detection and classification presented in this paper was implemented in four stages, as seen in Figure 2: pre-processing, processing, detection and classification.

During the pre-processing stage, the processor sends the control signals to the A/D and acquires N = 65536 samples [u_1, u_2, ..., u_N]. Meanwhile, the samples are transferred through DMA to the external memory every 4096 samples. When all N samples were acquired and stored in the SDRAM, the PQ analyzer proceeds to the next block in the pre-processing stage. While processing the recently acquired waveforms, the analyzer continues with the acquisition of the next cycle to ensure continuous monitoring of the power system.

During processing, a normalization block is used to necessary because it make the detection process (selection of threshold levels) independent of the voltage transducer's range. Once the signal is normalized, a first estimation of the waveform's frequency is calculated through the Fast Fourier Transform (FFT) and the Interpolated Discrete Fourier Transform (IpDFT) algorithms. Then its magnitude and frequency's final estimation are calculated through sine-fitting algorithms. In this step, the pre-processing stage is over and basic information about the waveform is known.

After pre-processing, the analyzer proceeds to the processing stage. In this step, the processing splits and two different sets of algorithms are applied to the normalized voltage signal in order to detect different power quality disturbances.

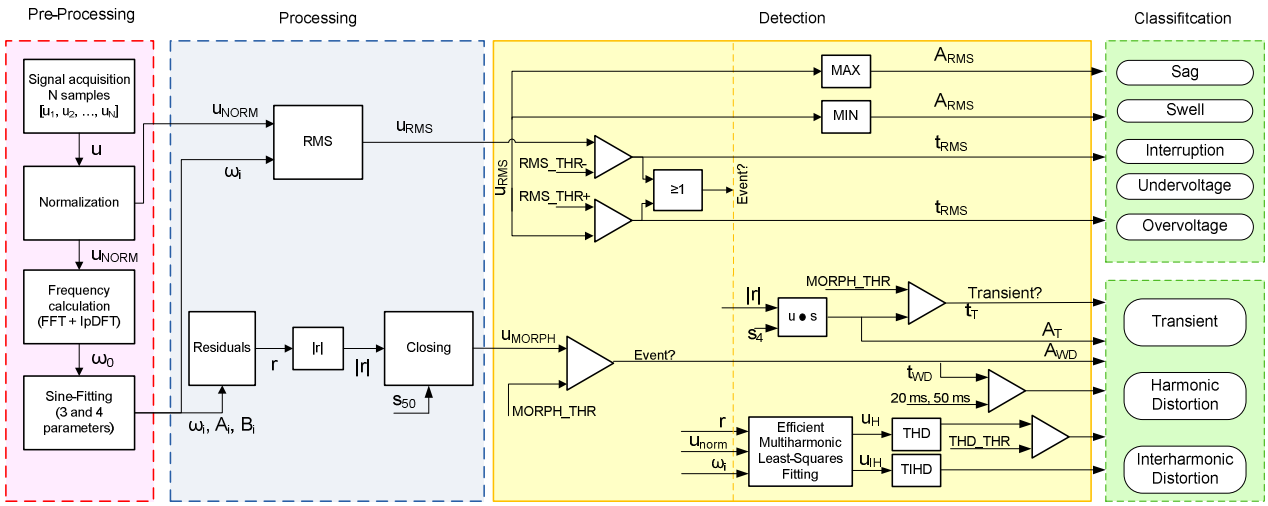

Figure 2 - Block diagram of the stages implemented in the PQ analyzer.

The upper branch deals with disturbances whose RMS value changes significantly. These disturbances are sags, swells, overvoltages, undervoltages and interruptions. The other set of algorithms are used to detect waveform distortions and transients. For these, the morphological operation closing was used to process discrete signals based on the signal shape but only after calculating the residuals. These are obtained by the difference of the acquired signal by the estimated signal. The residuals contain possible disturbances that have occurred as well all the harmonics (except the fundamental).

In the detection phase, the results obtained by the two algorithms are compared with the threshold values. If they're crossed an event is detected and then the classification of the disturbance occurred begins. Once the disturbance is detected, it's characteristics (type, duration, magnitude, …) are stored for later transmission to an external device.

A. Pre-processing stage: determining the frequency and the magnitude of the voltage signal

Since the instantaneous frequency is an indicator of great importance in time-varying signals, several algorithms have been developed for the determination of power quality disturbances knowing the frequency value [9]. A comparative study of methods was done taking into account the accuracy and number of operations, the execution speed and memory occupation employed by each method [10]. In this study, methods based on FFT (e.g. IpDFT [11]), Chirp-Z Transform, adaptive filters and methods based on Sine-Fitting algorithms [12] were compared. The purpose of this comparison was to determine the best method to be implemented on a DSP. According to [10], the IpDFT is the algorithm more precise, accurate and faster, thus it was the chosen algorithm for this work.

To determine the phase and magnitude of the acquired waveform, modified versions of the 3 and 4-parameter sine-fitting algorithms were implemented [13]. The first estimates the in-phase and quadrature components of the signal's magnitude, respectively, A_0 and B_0. With N normalized samples u_{NORM} [u_1, u_2, ..., u_N] acquired at instants [t_1, t_2, ..., t_N], the function that fits the acquired waveform is

$$u_n = A_0 \cos(\omega_0 t_n) + B_0 \sin(\omega_0 t_n) \tag{2}$$

where ω_0 is the frequency determined by the IpDFT algorithm. It can also be written as

$$u_n = D\cos(\omega_0 t_n + \theta) \tag{3}$$

where

$$D = \sqrt{A_0^2 + B_0^2} \tag{4}$$

and

$$\theta = -atan2(B_0, A_0). \tag{5}$$

The sine-fitting minimizes the sum of squared residuals

$$\sum_{n=1}^{N} \left[u_n - A_0 \cos(\omega_0 t_n) - B_0 \sin(\omega_0 t_n) \right]^2 \tag{6}$$

where the residuals are

$$r_n = u_n - A_0 \cos(\omega_0 t_n) - B_0 \sin(\omega_0 t_n). \tag{7}$$

Equation (6) can be expressed in its matricidal form given by

$$(\mathbf{u} - \mathbf{D_0} \cdot \mathbf{x_0})^T \cdot (\mathbf{u} - \mathbf{D_0} \cdot \mathbf{x_0}) \tag{8}$$

where the matrices $\mathbf{u}$, $\mathbf{D_0}$ and $\mathbf{x_0}$ are

$$\mathbf{D_0} = \begin{bmatrix} \cos(\omega_0 t_1) & \sin(\omega_0 t_1) \\ \cos(\omega_0 t_2) & \sin(\omega_0 t_2) \\ \bullet & \bullet \\ \bullet & \bullet \\ \cos(\omega_0 t_N) & \sin(\omega_0 t_N) \end{bmatrix}_{Nx2} \tag{9}$$

$$\mathbf{u} = \begin{bmatrix} y_1 & y_2 & \bullet & \bullet & y_N \end{bmatrix}^T \tag{10}$$

and

$$\mathbf{x_0} = \begin{bmatrix} A_0 \\ B_0 \end{bmatrix}. \tag{11}$$

To determine A_0 and B_0 one must proceed to the calculation of

$$\mathbf{x}_0 = (\mathbf{D}_0^T \mathbf{D}_0)^{-1} \mathbf{D}_0^T \mathbf{u} \,. \tag{12}$$

The 4-parameter sine-fitting uses an iterative process to find the values of A_i, B_i and ω_i, that minimize the sum of squared differences. ω_i is the frequency applied to the waveform recorder input given by

$$\omega_i = \omega_{i-1} + \Delta\omega_i \tag{13}$$

where $\Delta\omega_0 = 0$. The matrices $\mathbf{D_0}$ and $\mathbf{x_0}$ are

$$\mathbf{D_i} = \begin{bmatrix} \cos(\omega_i t_1) & \sin(\omega_i t_1) & \alpha_{i,1} \\ \bullet & \bullet & \bullet \\ \bullet & \bullet & \bullet \\ \cos(\omega_i t_N) & \sin(\omega_i t_N) & \alpha_{i,N} \end{bmatrix}_{Nx3} \tag{14}$$

and

$$\mathbf{x_i} = \begin{bmatrix} A_i \\ B_i \\ \Delta\omega_i \end{bmatrix}. \tag{15}$$

where

$$\alpha_{i,n} = -A_{i-1} t_n \sin(\omega_i t_n) + B_{i-1} t_n \sin(\omega_i t_n) \tag{16}$$

The algorithm stops when the RMS value of the residuals is less than a predefined threshold value. Another approach is to define a maximum number of iterations or to define a stop condition: the algorithm stops when $|\Delta\omega_i / \omega_i|$ is below a determined threshold level (*e.g.,* 10^{-7}) [14].

B. *Detection of transients and waveform distortions: processing and detection stages*

In order to detect transients and waveform distortions, the fundamental u_F and the non-fundamental r components of the voltage signal u_{NORM} have to be separated

$$u_{NORM} = u_F + r \tag{17}$$

where r are the residuals obtained from the modified 4-parameter sine-fitting algorithm. The residuals contain the potential disturbances. Before the closing operation, the absolute value of r is calculated.

The mathematical operation closing [15] is a morphological operation and it's used to process discrete signals based on their shape,

$$u_{MORPH} = |r| \bullet s_{50} \tag{18}$$

where s_{50} is the structuring element. The structuring element is a binary vector whose length, N_{S50}, is equal to 2.5 times the nominal period (20 ms). If the A/D is sampling at f_S=25.6 S/s and the network frequency is 50 Hz, a period corresponds to 512 acquired samples. In this way, N_{S50} = 2.5*512=1280.

According to the definition, the closing operation was implemented using two other morphology operations: dilation and erosion. Both were implemented using the van Herk-Gil-Werman algorithm [16][17] and each sample requires 3-4/N_S comparison perations. The resulting signal u_{MORPH} is an envelope of the signal |r|. Calculating the envelope simplifies the detection of potential events using thresholding because it removes multiple crossings of the threshold level that belong to a single event. An event is detected when the signal u_{MORPH} crosses the threshold level *MORPH_THR*.

In the detection step, the detected events are classified based on their parameters such as duration and the content of harmonic and interharmonic frequencies. If the duration of the event (t_{WD}) is longer than 50 ms or the duration is longer than 20 ms and, at the same time, the maximum THD exceeded THD_THR, the event is classified as waveform distortion, or, otherwise, classified as a transient.

In order to calculate the THD and TIHD values, the analyzer uses an innovative efficient implementation of multiharmonic least-squares fitting algorithm [18] to estimate the amplitudes of individual harmonics up to the 30th. Using the estimated parameters, *i.e.*, the estimated harmonics, the THD and TIHD values are calculated

$$\mathrm{THD} = \sqrt{\frac{\sum_{h=2}^{30}(A_h^2 + B_h^2)}{A_1^2 + B_1^2}} \tag{19}$$

$$\mathrm{TIHD} = \sqrt{\frac{1}{N}\sum_{n=0}^{N-1} u_{IH}{}^2[n]} \tag{20}$$

where A_h and B_h are respectively the in-phase and quadrature components of the hth harmonic, A_1 and B_1 are the in-phase an quadrature components of the fundamental and u_{IH} is

$$u_{IH} = u_{NORM} - \sum_{h=1}^{30} A_h \cos(h\omega_i t_n) - B_h \sin(h\omega_i t_n) \tag{21}$$

The magnitude A_{WD} of a waveform distortion is calculated as the maximum value of the signal u_{MORPH} during the event.

When a transient is detected, the analyzer processes, once again, the signal |r| using the closing operation but, this time, the structuring element is 4 ms long, which corresponds to N_{S4}=102. Shorter structuring element enables to separate potential transients that are close to each other in the signal $u_{MORPH.}$. The resulting signal is used to calculate the duration t_T and the magnitude of the individual transients A_T.

C. *Detection of sags, swells, interruptions, undervoltages and overvoltages: processing and detection stages*

The disturbances detection process of the first branch (sags, swells, interruptions, undervoltages and overvoltages) follows the recommendations of power quality standards and is based on the detection of variation of the voltage signal's RMS value

$$u_{RMS} = \sqrt{\frac{1}{N}\sum_{n=0}^{N-1} u_{NORM}^2[n]}\,. \tag{22}$$

The RMS value is calculated over one period of the power system's voltage and refreshed every half-period. The disturbance detection is done by comparing the RMS values with two threshold levels: *RMS_THR+* which is above the nominal RMS of the powler system and *RMS_THR-* which is below the nominal value. In the detection stage the magnitude A_{RMS} and the duration T_{RMS} are determined.

If an event had magnitude below 0.1 p.u., then is classified as transient. If the event's magnitude is above 0.1 p.u. and below *RMS_THR-*, the event is classified as sag or undervoltage (depending on its duration). Otherwise (i.e. when the event's magnitude is above *RMS_THR+*), the event is classified as either swell or overvoltage. These conditions are illustrated in Figure 3.

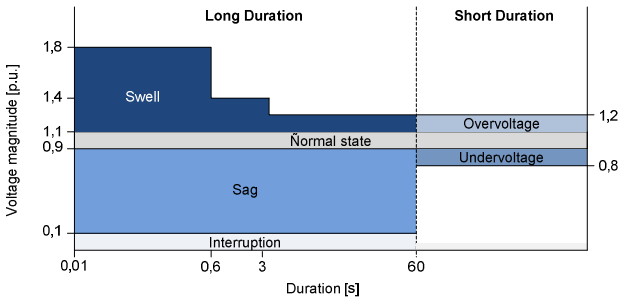

Figure 3 – Disturbance duration vs. voltage RMS value characteristics of typical short and long duration PQ disturbances.

IV. MEASUREMENT RESULTS

The prototype of the analyzer was connected and installed at Instituto Superior Técnico, Oeiras, where it monitored the local condition of the power system. The *MORPH_THR* threshold was set to 0.12 p.u., the *RMS_THR+* was set to 1.1 p.u. and the threshold *RMS_THR-* was adjusted to 0.9 p.u.

Since disturbances whose RMS changes aren't often, some were simulated so that the algorithms implemented could be validated.

Figure 4 and Figure 5 show an example of a detected interruption (duration 0.29 s, minimum magnitude 0.004 p.u.). The disturbance began at 9h31m54.23s and finished at 9h31h54.52s, on March 21, 2011.

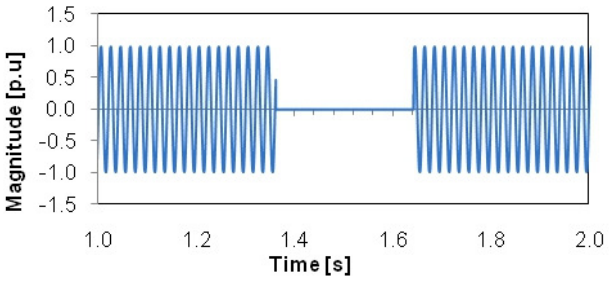

Figure 4 – Interruption:voltage signal.

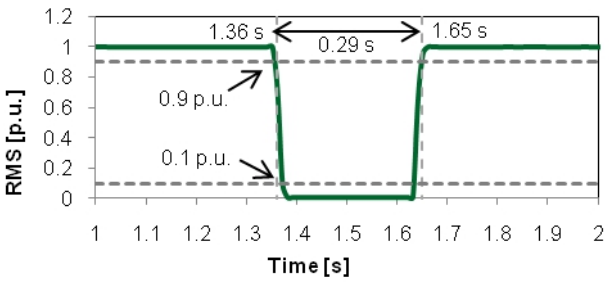

Figure 5 – Interruption: RMS variation.

A detected swell is shown in Figure 6 and Figure 7. It began at 9h43m26.43s and finished at 9h43h26.40s (duration 0.08 s, maximum magnitude 1.247 p.u.) on March 21, 2011. The RMS variation is shown in Figure 13.

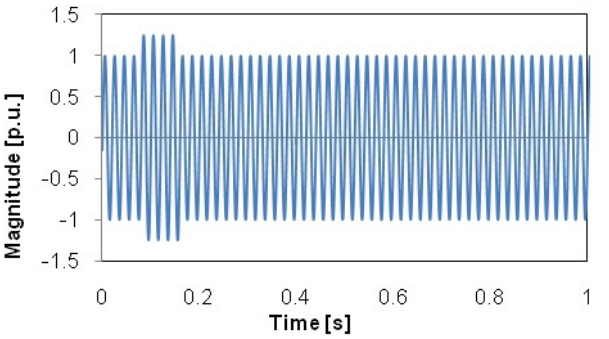

Figure 6 – Swell: voltage signal.

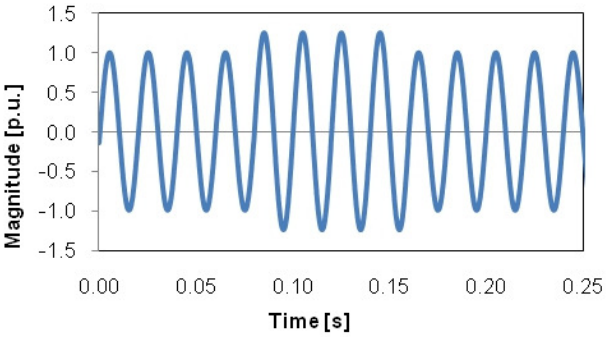

Figure 7 – Swell: voltage signal (detail).

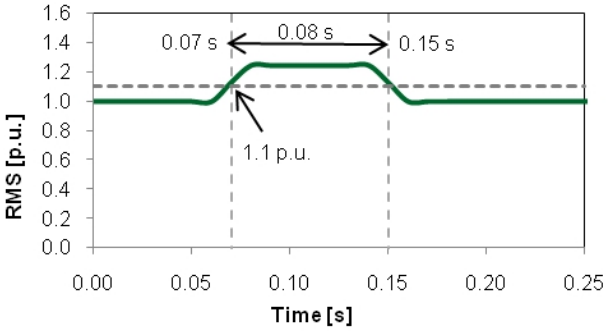

Figure 8 – Swell: RMS variation.

A sag was simulated and detected on March 21, 2011 (duration 0.12 s, minimum value 0.665 p.u.), as illustrated in Figure 9, Figure 10 and Figure 11).

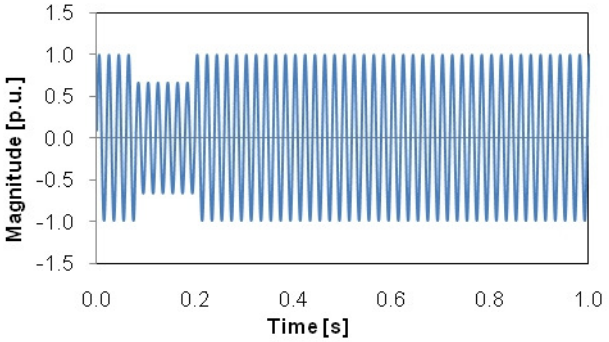

Figure 9 – Sag: voltage signal.

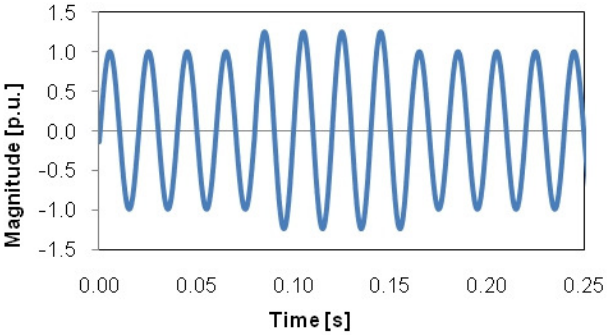

Figure 10 – Sag: voltage signal (detail).

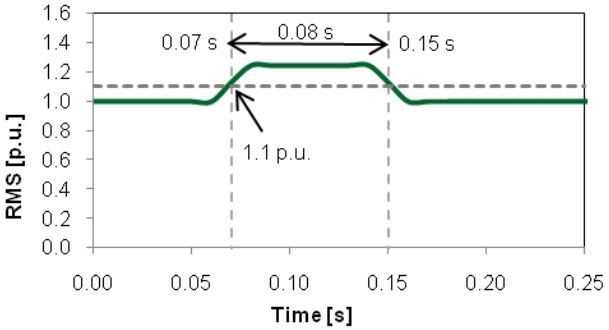

Figure 11 – Sag: RMS variation.

Figure 12 depicts a waveform distortion on the voltage signal. The residuals are shown in Figure 13 and the result of the morphological operation closing in Figure 14.

It can be seen that at 0.208 s the morph result crosses *MORPH_THR* and stays above 0.12 p.u. for 0,0596 s.

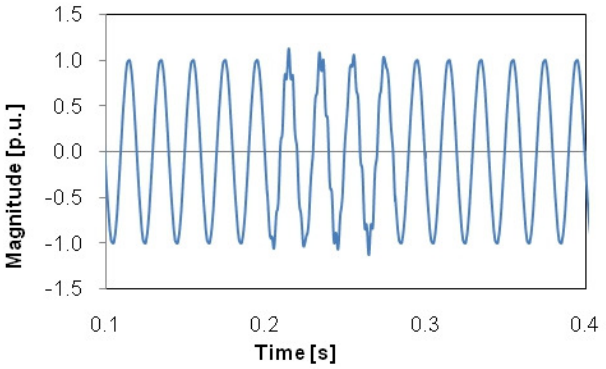

Figure 12 – Waveform distortion: voltage signal.

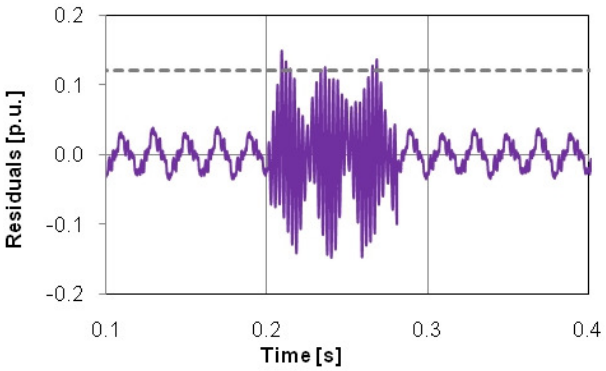

Figure 13 – Waveform distortion: residuals.

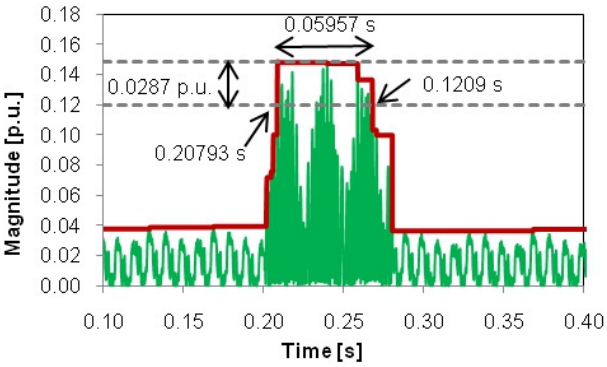

Figure 14 – Waveform distortion: morphology result.

Finally a transient was detected on March 19, 2011 at 15h33m24.43s, with duration 78.2 µs and magnitude 0,485 p.u.. The transient is depicted in Figure 20 and Figure 21.

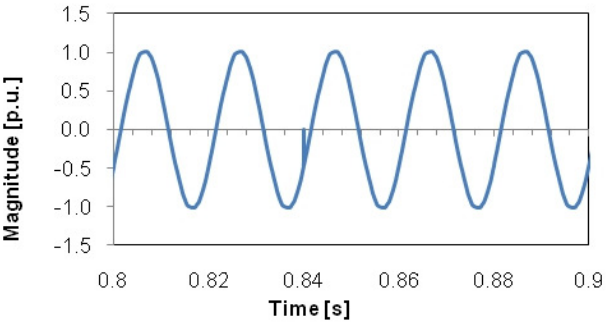

Figure 20 – Transient: voltage signal.

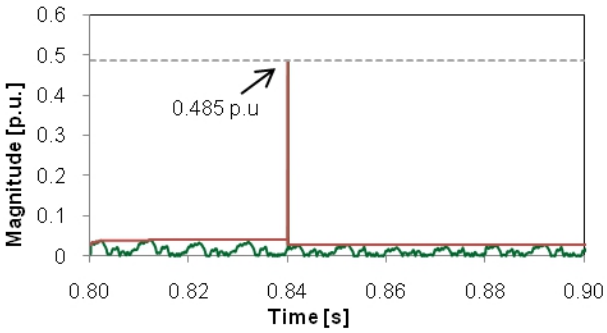

Figure 21 – Transient: morphology result.

V. CONCLUSIONS

The designed prototype of a power quality analyzer implements two groups of different algorithms. For transients and waveform distortions, sine-fitting and mathematical operation closing are applied. Disturbances from the second group (*e.g.*, sags, swells and interruptions) are detected and classified using the voltage RMS value. The mathematical operations are usually used in image processing. This paper shows that they can represent a useful and efficient tool also in power quality measurements.

The proposed method was tested using both simulated data with artificial disturbances and data measured in a single-phase power system. All algorithms used for detection and classification are fast, simple, and suitable for implementation on a DSP. An advantage of the proposed method is the simplicity of adjustment of its sensitivity: by adjusting the threshold levels *MORPH_THR* and *RMS_THR*, its sensitivity can be adjusted to the required level.

The drawbacks of the method lie in its inability to measure high frequency transients, due to the bandwidth of the voltage transducer.

The analyzer is based on a digital signal processor ADSP-21369. The analyzer is able to perform all the required processing in real-time and is therefore suitable for real-time monitoring of the power system. Its performance was tested when monitoring a single-phase power system.

REFERENCES

[1] Entidade Reguladora dos Serviços Energéticos. ERSE. [Online]. http://www.erse.pt/

[2] "IEEE Std. 1159TM-2009 (revision of IEEE Std 1150-1995)," *IEEE Recommended Practice for Monitoring Electric Power Quality, The Institute of Electrical and Electronics Engineers, Inc., New York*, June 2009.

[3] Zwe-Lee Gaing, "Wavelet-based Neural Network for Power Quality Disturbance Recognition and Classification," *IEEE Transactions on Power Delivery*, vol. 19, issue 4, pp. 1560–1568, Oct. 2004.

[4] Min Wang, G. I. Rowe, and A. V. Mamishev, "Classification of Power Quality Events Using Optimal Time-Frequency Representations – Theory and Application," *IEEE Transactions on Power Delivery*, vol. 9, issue 3, pp. 1488-1503, Jul. 2004.

[5] A. M. Gaouda, S. H. Kanoun, M. M. A. Salama, and A. Y. Chikhani, "Pattern Recognition Applications for Power System Disturbance Classification," *IEEE Transactions on Power Delivery*, vol. 17, issue 3, pp. 677–683, Jul. 2002.

[6] Feng-Feng Zhu, Guo-Sheng Hu, and Jing Xie, "Classification of Power Quality Disturbances Using Wavelet and Fuzzy Support Vector Machines," *Proceedings of 2005 International Conference on Machine Learning and Cybernetics*, vol. 7, pp. 3981–3984, Aug 2005.

[7] Z. Chen and P. Urwin, "Power Quality Detection and Classification Using Digital Filters," *2001 IEEE Porto Power Tech Proceedings*, vol. 1, no. 6, p. 6, Sept. 2001.

[8] E. Styvaktakis, M. H. J. Bollen, and I. Y. H. Gu, "Automatic Classification of Power System Events Using RMS Voltage Measurements," *2002 IEEE Power Engineering Society Summer Meeting*, vol. 2, pp. 824–829, Jul. 2002.

[9] D. Castaldo, D. Gallo, C. Landi, and A. Testa, "A digital instrument for nonstationary disturbance analysis in power lines," *IEEE Trans. on Instr. and Meas.*, vol. 53, nº 5, pp. 1353-1361, Oct. 2004.

[10] Pedro M. Ramos and A. Cruz Serra, "Comparison of Frequency Estimation Algorithms for Power Quality Assessment," *Journal of the International Measurement Confederation (IMEKO)*, vol. 42, pp. 1312-1317, May 2008.

[11] J. Schoukens, R. Pintelon, and H. Van hamme, "The Interpolated Fast Fourier Transform: A Comparative Study," *IEEE Trans. on Instr. and Meas.*, vol. 41, nº 2, pp. 226-232, Apr. 1992.

[12] D. Agrez, "Frequency estimation of the non-stationary Signals Using interpolated DFT," *IMTC/2002*, vol. 2, pp. 925-930, May 2002.

[13] "IEEE Standard for Digitizing Waveform Recorders (IEEE Std 1057-1994 (R2001))," *Waveform Measurements and Analysis Committee of the IEEE Instrumentation and Measurement Society*, 2001.

[14] Pedro M. Ramos, Tomás Radil, and Fernando M. Janeiro, "Sine-Fitting Algorithms Implemented in 32-bit Floating Point Systems," *Instrumentation for the ICT - 17th Sympoium IMEKO TC 4, 3rd Symposium IMEKO TC 19 and 15th IWADC Workshop, Kosice, Slovakia*, pp. 8-10, Sept. 2010.

[15] J. Serra, *Image Analysis and Mathematical Morphology*. New York: Academic, 1982, vol. 1.

[16] M. van Herk, "A fast algorithm for local minimum and maximum filters on rectangular and octogonal kernels," *Pattern Recognition Letters*, vol. 13, pp. 517-521, Jul. 1992.

[17] J. Y. Gil and M. Werman, "Computing 2-D min, median and max filters," *IEEE Trans. Pattern Analysis and Machine Intelligence*, vol. 15, nº5 , pp. 504-507, May 1993.

[18] Pedro E. Xavier, Pedro M. Ramos, and Fernando M. Janeiro, "Efficient Implementation of Multiharmonic Least-Squares Fitting Algorithms," p. 2, Março 2011.